

---

# A Short-term PV Power Prediction and Uncertainty Analysis Model Based on CEEMDAN and AHA-BP

---

Zhiyuan Zeng<sup>1</sup>, Tianyou Li<sup>1,2,\*</sup>, Jun Su<sup>1,2</sup>,  
Yihan Yang<sup>1</sup> and Yajun Lin<sup>1</sup>

<sup>1</sup>*School of Electrical Engineering and Automation, Xiamen University of Technology, Xiamen, China*

<sup>2</sup>*Xiamen Key Laboratory of Frontier Electric Power Equipment and Intelligent Control, Xiamen, China*

*E-mail: 2019000005@xmut.edu.cn*

*\*Corresponding Author*

Received 28 May 2024; Accepted 19 July 2024

## Abstract

The stochastic and intermittent nature of photovoltaic (PV) generation brings a series of scheduling problems to the power system. An effective prediction of PV power is essential to minimize the impact of uncertainty. Therefore, this paper presents an integrated prediction model with complete ensemble empirical mode decomposition with adaptive noise (CEEMDAN), the artificial hummingbird algorithm (AHA), and the BP neural network (BPNN) for predicting power generation from PV power plants, and a methodology for uncertainty analysis by using the nonparametric kernel density estimation (NPKDE). First, one month of PV power is decomposed into an array of components using CEEMDAN. Then, the weights and thresholds of the BPNN are optimized by using AHA. These components are trained using the BPNN. Finally, the final prediction results are obtained by superimposing the components, and NPKDE is employed to compute the probability density

*Distributed Generation & Alternative Energy Journal, Vol. 39\_4, 875–898.*

doi: 10.13052/dgaej2156-3306.3949

© 2024 River Publishers

and confidence interval of the prediction error. The proposed prediction method demonstrates superior predictive performance in comparison with other models. Also, the NPKDE approach better describes the accuracy of the probability density distribution.

**Keywords:** PV power prediction, CEEMDAN, artificial hummingbird algorithm, BP neural network, Kernel density estimation, confidence interval.

## 1 Introduction

Recently, the escalating inclination to mitigate fossil fuel consumption and address ecological issues has propelled technological innovations aimed at the development and utilization of renewable energy sources [1, 2]. PV power generation reduces the usage of traditional energy sources throughout the energy transition and, at the same time, brings challenges to grid power distribution [3]. However, weather variations and seasonal changes can change unpredictable meteorological factors such as temperature, humidity, irradiance, etc., resulting in the stochastic and intermittent behaviour observed in PV power generation [1, 4]. The unpredictability inherent in this stochastic characteristic can have an immense effect on the power system's reliability.

Under the time scale of prediction, numerous theories and techniques for PV power prediction are currently being researched. These are categorized into three categories: long-term, medium-term, and short-term predictions [5]. For real-time scheduling and operations management of renewable energy generation systems, short-term PV prediction is the most appropriate among the methods. This prediction provides a more precise estimate of PV power generation over a short period of time, which helps to optimize the charging and discharging strategies of photovoltaic-energy storage systems (PV-ESS) to cope with fluctuations in power demand and changes in market prices, thus improving energy efficiency and reducing operating costs [6, 7]. Such short-term PV prediction holds immense importance in the scheduling of traditional power systems as well as PV-ESS [8, 9].

In the PV prediction problem, the mainstream methods for predicting PV power consisted of indirect prediction utilizing physical models and direct prediction relying on historical data [10]. The historical data-based forecasting methods consist of neural networks, time series and support vector machines. The neural network has been recognized as an excellent prediction method, and its extensive use in the power prediction field has

become increasingly crucial. Most of the existing research focused on two major areas: one is the use of neural network algorithms themselves for power prediction, and the other one is the optimization of neural networks using algorithms [11]. Neural networks possess significant self-learning capabilities. However, they are susceptible to converging on local optima [12]. The application of optimization algorithms can effectively address this issue. In [13], for enhanced precision, the weights and thresholds of the BP neural network (BPNN) were optimized using the genetic algorithm (GA) and particle swarm optimization (PSO). These algorithms optimize the BPNN to reduce the prediction model's error level significantly.

With science and technology developing at a rapid pace, many new algorithms have emerged. The artificial hummingbird algorithm (AHA) [14], an emerging bioinspired optimization algorithm, has been widely noticed and applied for its broad applicability and fast search speed. In [15], this paper takes advantage of the long-time memory artificial hummingbird algorithm (LMAHA) to optimize the energy management of wind-energy storage systems. The findings indicate the method can actively cope with the forecasting challenges regarding load and power uncertainty. In addition, the algorithm can not only enhanced prediction accuracy [16], but also optimized the optimal current allocation of the power system, resulting in stable and efficient operation [17]. Hence, this paper employs the AHA to enhance the predictive model.

However, the BPNN prediction results are not satisfied when dealing with stochastic fluctuation signals. While the empirical modal decomposition (EMD) method can decompose stable signals to improve prediction accuracy, it often faces the signal decomposition issue of modal aliasing [18, 19]. In order to tackle this issue, the complete ensemble empirical mode decomposition with adaptive noise (CEEMDAN) method features an achievable solution for mitigating the modal aliasing phenomenon. In [20], the wind power data was decomposed using CEEMDAN. Based on the properties of the decomposed data, a grey wolf optimization-bidirectional long short-term memory network (GWO-Bi LSTM) prediction model was established. The results show the model is superior at predicting short-term wind power prediction.

Although PV power prediction has been of interest to researchers and scholars in this field, PV power generation is weather-dependent, which leads to a certain degree of uncertainty in PV power. Thus, it is imperative to comprehend the uncertainty of PV changes and to predict and assess them with precision. Uncertainty analysis of PV power prediction can be

done using parametric and nonparametric methods [21]. The parametric method requires assumptions about the prediction error distribution, such as Gaussian distribution and Beta distribution [22]. Nonparametric methods include kernel density estimation (KDE) [23], Bootstrap, etc. Among them, KDE can flexibly adapt to various data types and complexity and generate intuitive and precise density estimation curves for visualization and analysis, which is widely used. The nonparametric kernel density estimation (NPKDE) can be utilized to compute the distribution of PV power prediction errors without assuming error distribution, which can provide a more comprehensive understanding of the stability and reliability of the outcomes of the prediction [24]. Therefore, the nonparametric method is chosen for this paper.

This present study introduces an innovative approach for PV power prediction and uncertainty analysis methods based on CEEMDAN, AHA, BP, and NPKDE. This paper has the following main contributions:

- A CEEMDAN-based PV power prediction model which decomposes and reconstructs the single to improve the accuracy of the prediction;
- A BPNN model optimizes its thresholds and weights using the AHA algorithm, which raises the prediction model's accuracy;
- Uncertainty in PV power prediction is analyzed with NPKDE.

The remainder of this study is structured below. In Section 2, the AHA-BP structure is introduced along with the theoretical foundation of CEEMDAN. After analyzing the data, Section 3 presents the evaluation indexes and parameter setting of the prediction model, and validates the proposed model. Section 4 analyzes the uncertainty of PV power prediction. Finally, conclusions and shortcomings are drawn.

## 2 Theoretical Background

### 2.1 CEEMDAN

EMD is a time-frequency preprocessing analytical method [25], which is widely used in many projects such as earth dam health monitoring [26], irradiance prediction [27] and carbon price prediction [28]. The single is decomposed into a series of intrinsic mode functions (IMF) and a residual signal (RES) that represents the trend of the sequence. Since EMD generates a mixed-modal problem, the CEEMDAN can provide an effective way to overcome this problem [29]. The major steps of decomposition are listed below:

1. Add the Gaussian white noise to the original signal  $x(t)$ :

$$x_i(t) = x(t) + \varepsilon_0 \omega_i(t) \quad i = 1, 2, 3, \dots, k \quad (1)$$

where  $\varepsilon_k$  is the signal to noise ratio (SNR), and  $\omega_i(t)$  represents Gaussian white noise,  $i$  is the  $i$ th addition of white noise.

2. The signals after adding noise were decomposed by using the EMD to obtain the first  $IMF_1$  and  $RES$ .

$$RES_1(t) = x(t) - IMF_1(t) \quad (2)$$

3. Add noise to the first  $RES$  and continue to use EMD to obtain the new  $IMF$ .
4. Finally, the following can be used to express the result of CEEMDAN's decomposition:

$$IMF_n(t) = \frac{1}{k} \sum_{i=1}^k E_1(r_{n-1}(t) + \varepsilon_1 E_{n-1}(\omega_i t)) \quad n = 2, 3, \dots, k \quad (3)$$

$$RES_n(t) = RES_{n-1}(t) - IMF_n(t) \quad (4)$$

$$x(t) = \sum_{i=1}^n IMF_n(t) + RES(t) \quad (5)$$

where,  $n$  is the total amount of components,  $E_{n-1}(\cdot)$  is the  $n-1$ th IMF.

## 2.2 AHA

The main focus of the AHA algorithm is to imitate the behaviour of hummingbirds feeding on nectar. The fitness function, which indicates the quality of the food source, can be used to describe the nectar filling rate of the food source [30]. Hummingbirds foraging behaviour consists of three stages: guided foraging, territorial foraging, and migration foraging [31]. Hummingbirds have three types of flight: axial, diagonal and omnidirectional, as shown in Table 1.

Where  $randi([1, d])$  represents the generation of a random integer between  $[1, d]$ ,  $rankperm(k)$  represents the generation of a random  $k$  integers between  $[1, d]$ ,  $r_1$  represents a random number in  $(0, 1)$ .

Hummingbirds will utilize three flight skills during their foraging. The following are the three foraging behaviours of hummingbirds, as shown in Table 2.

**Table 1** Three types of flight

Type	Formula	
Axial Flight	$D^{(i)} = \begin{cases} 1 & i = randi([1, d]) \\ 0 & else \end{cases} \quad i = 1, \dots, d$	(6)
Diagonal Flight	$D^{(i)} = \begin{cases} 1 & \text{if } i = P(j)j \in [1, k]P \\ & = rankperm(k)k \in [2, [r_1 \cdot (d - 2)] + 1] \\ 0 & else \end{cases}$	(7)
Omnidirectional Flight	$D^{(i)} = 1 \quad i = 1, \dots, d$	(8)

**Table 2** Foraging behaviours

Type	Formula	
Guided Foraging	$v_i(t + 1) = x_{i,tar}(t) + a \cdot D \cdot [x_i(t) - x_{i,tar}(t)]$	(9)
Territorial Foraging	$v_i(t + 1) = x_i(t) + b \cdot D \cdot x_i(t)$	(10)
Migration Foraging	$x_{wor}(t + 1) = Low + r \cdot (Up - low)$	(11)

Where  $x_i(t)$  represents the location of the target food source at the  $t$ th iteration;  $x_{i,tar}(t)$  is the target food source location that the  $i$ th hummingbird plans to visit; and  $a$  is a bootstrapping factor obeying a standard normal distribution;  $b$  is the flight step length;  $x_{wor}$  is the deprived food source in the population,  $Up$  represents the upper boundary, while  $Low$  represents the lower boundary.

When the food is scarce, the hummingbird will fly farther away to search for new food sources. If hummingbirds reach a tiny food source and the iteration time surpasses the pre-established migration coefficient value. The hummingbirds will give up on that food source and randomly select a new one in the search space.

### 2.3 AHA-BP

The BPNN consists of three layers: input, hidden and output[32]. Figure 1 illustrates the model's unique procedure and steps:

- Determine the BPNN structure: initialize the weights and thresholds of the BPNN. Initialize the relevant parameters of AHA, the population and construct the visit table;
- Select hummingbird's behaviour: select hummingbird's flight mode and foraging mode and calculate candidate food source fitness;
- Update hummingbird's position and visit table: according to the foraging rules and the current position of hummingbirds, the position

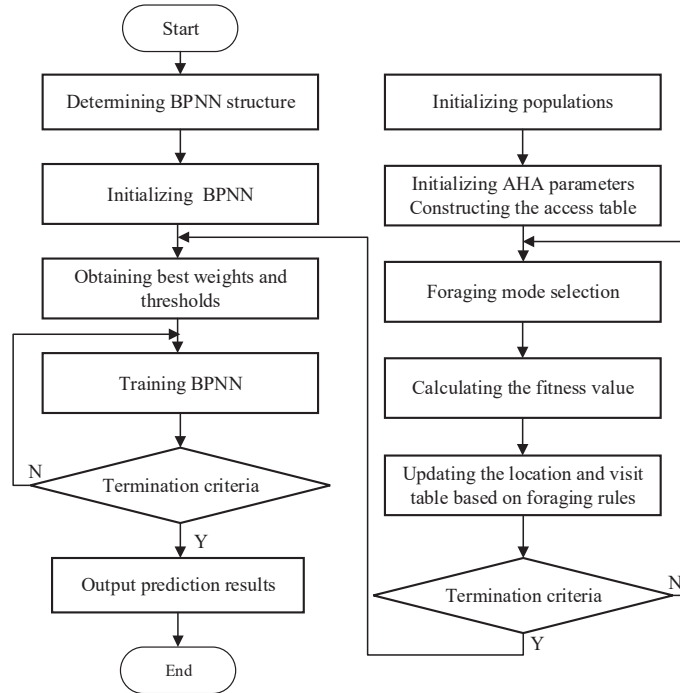


**Figure 1** AHA-BP flow chart.

of hummingbirds and visit table are updated, and if the condition of migratory foraging is reached, migratory foraging is carried out. Repeat the calculation of adaptation until the maximum number of iterations is achieved;

- Output the best result: for each hummingbird location, calculate the value of the fitness function, which is measured by the error of BPNN on the training data. After reaching the number of iterations, the current optimal fitness is assigned to the BPNN;
- Train the neural network: based on the optimal weights and thresholds obtained by AHA, train the neural network to predict the samples. The prediction results are output when the cutoff conditions are satisfied.

## 2.4 CEEMDAN-AHA-BP Hybrid Prediction Model

This study suggests a technique for predicting PV power by integrating CEEMDAN with AHA-BP. The CEEMDAN decomposes the PV power

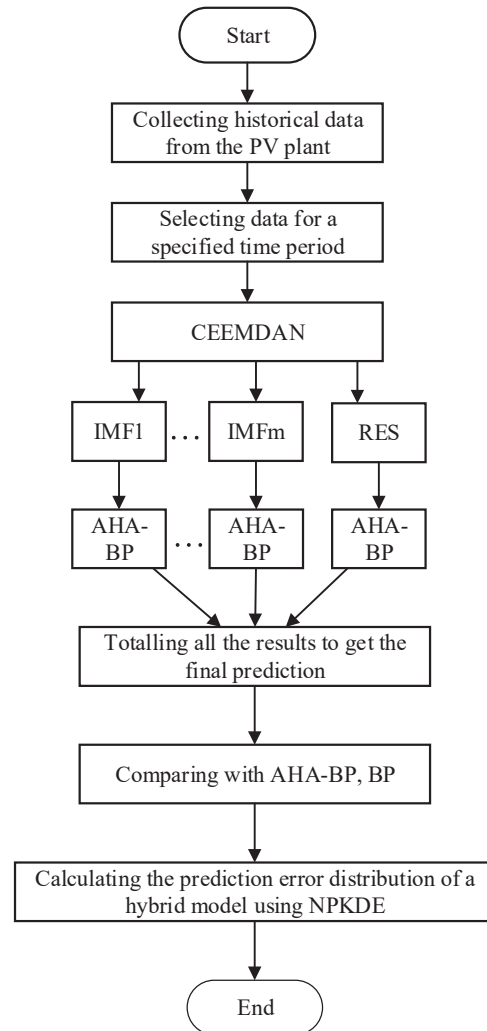


**Figure 2** Predictive model flow chart.

into multiple IMFs components from high to low frequency and RES. And AHA-BP processes each component of the CEEMDAN.

The steps of the model are displayed in Figure 2:

- Collect the historical data pertaining to the PV plant. Since PV plant does not generate electricity throughout the day, the time period of PV generation is selected;



- Decompose into IMF components and RES using CEEMDAN;
- Split the results of each component into a training and test set, and input the meteorological factors into the AHA-BPNN model to train;
- The ultimate prediction values are derived by summarizing the prediction outcomes of each component and comparing them with other prediction models to confirm the accuracy of the prediction of this hybrid model;
- Calculate the prediction error distribution of the prediction model using NPKDE and confirm its efficiency.

To examine the prediction model, various assessment metrics are typically employed. In this paper, three indicators coefficient of determination ( $R^2$ ), Root Mean Square Error (RMSE), and Mean Absolute Error (MAE) are used [33]. The formulas for  $R^2$ , RMSE, and MAE are shown by the following Table 3.

**Table 3** Concept of assessment indicators

Measure	Formula	Judgment
$R^2$	$R^2 = 1 - \frac{\sum_i (\hat{y}_i - y_i)^2}{\sum_i (\bar{y}_i - y_i)^2}$	The higher its value is, the better it is.
RMSE	$RMSE = \sqrt{\frac{1}{m} \sum_{i=1}^m (\hat{y}_i - y_i)^2}$	The larger the error, the larger the value.
MAE	$MAE = \frac{100\%}{m} \sum_{i=1}^m  \hat{y}_i - y_i $	

where  $\hat{y}_i$  is the predicted value,  $y_i$  is the true value,  $\bar{y}_i$  is the mean value.

### 3 Case Study

#### 3.1 Data Collection Platform

The data came from a PV power plant of an industrial user in Xiamen, Fujian Province, China. The meteorological data are obtained from the weather station of the PV power plant. Figures 3 and 4 display the user interface of the PV power station and the interface of the environmental platform.

The installed capacity of this PV plant is 309.32 kWp. In this paper, the historical PV power and irradiance for the month of December 2022 is selected as a case study. Considering the characteristic of the PV power plant that the output power is zero at night, the prediction time period is

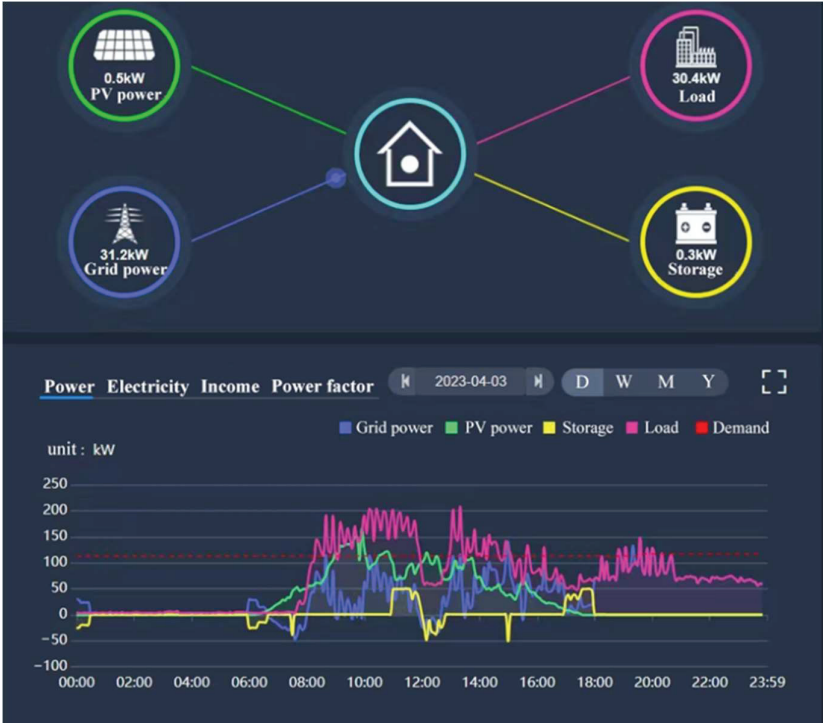


Figure 3 User interface.

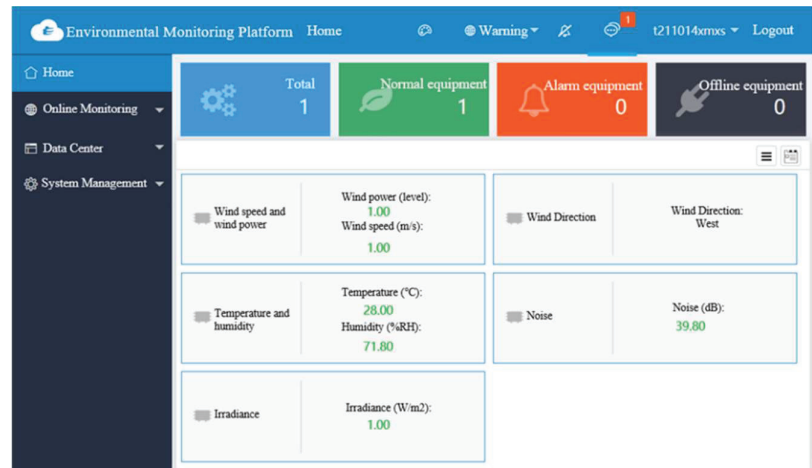
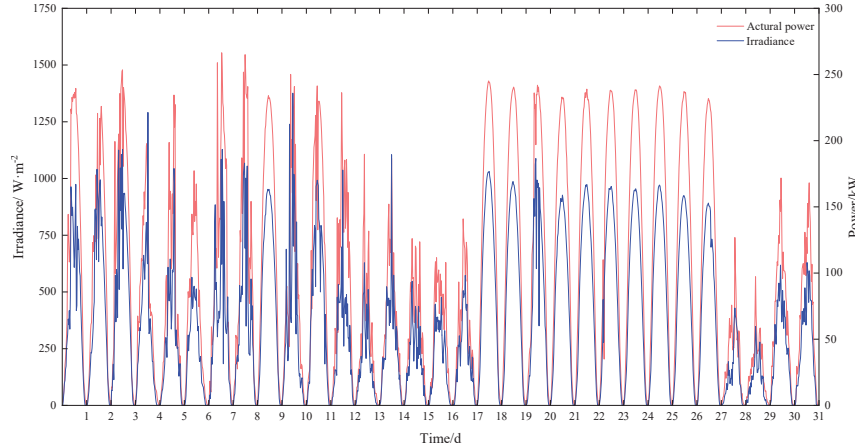


Figure 4 Environmental monitoring interface.



**Figure 5** Comparison between PV power generation and irradiance curves.

limited to 7:00 to 18:00 every day. Figure 5 illustrates the collected data for the PV power and irradiance profiles for various weather conditions over a one-month period.

### 3.2 CEEMDAN Decomposition

The power series of the selected dataset are decomposed using CEEMDAN. And the IMF and RES are displayed in Figure 6.

The data presented in Figure 6 reveals that the frequency decreases, the individual component signal curves behave more stably, and their periodicity becomes clearer. Among them, IMF1 to IMF4 show non-periodic variations, while they exhibit higher frequency and relatively sharp fluctuations, which reflects the stochastic character of PV power. In addition, the changes from IMF5 to IMF10 show a certain periodicity. These components with periodic patterns have a high impact on the prediction accuracy, and their amplitude varies greatly, leading to a more pronounced effect on the final prediction outcomes.

### 3.3 Comparative Analysis of Prediction Models

All of the models presented in this research are implemented using MATLAB 2022b. The results of IMFs and RES components after using CEEMDAN are separated into training and test sets. The meteorological factors are input into the AHA-BPNN model to make a prediction, and the total of each

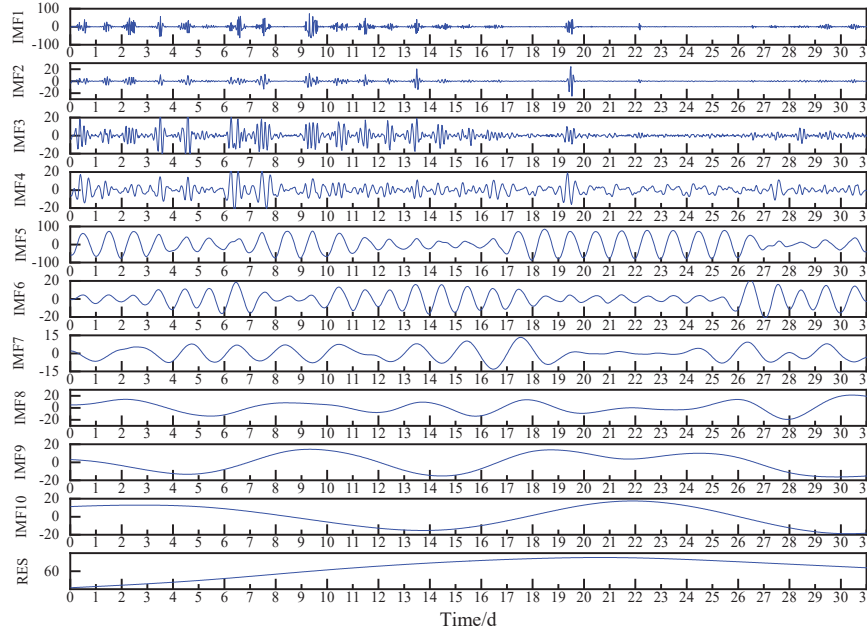


**Figure 6** Decomposition result of CEEMDAN.

component's prediction outcomes is the final prediction result. The results are shown in Figure 7 below.

From Figure 7, it is observed that compared with other prediction models, the CEEMDAN-AHA-BP prediction model has a better fit to reality, underscoring the exceptional level of accuracy of the integrated prediction model. The integrated prediction model outperforms the single prediction model as compared to the BPNN model. This demonstrates that the prediction model incorporating signal decomposition outperforms the BPNN prediction model optimized using the optimization algorithm and also highlights the superiority of the AHA over the PSO. It is worth noting that it can be effective in decreasing the fluctuation of PV power generation signals, while CEEMDAN performs better in terms of decomposition effect compared to EMD.

By comparing and analyzing these indicators, the predictive performance of the models can be assessed more comprehensively, and thus, the optimal model can be identified. Table 4 describes the performance the performance evaluation between the various models as well as the results of MAE, RMSE and  $R^2$ . It also shows the performance of EMD-AHA-BP, AHA-BP, PSO-BP and BP.

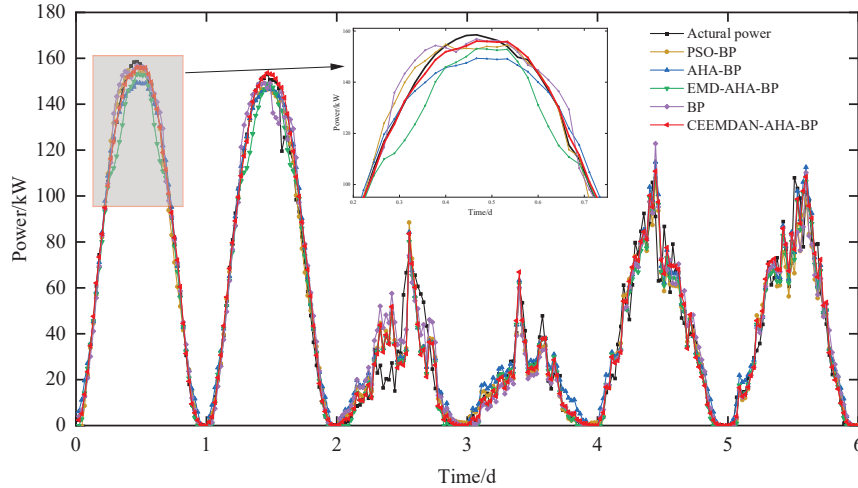


**Figure 7** Final forecasting results.

**Table 4** Predicted indicator results

Prediction Model	$R^2$	RMSE	MAE
BP	0.9627	9.110	6.321
PSO-BP	0.9686	8.402	5.954
AHA-BP	0.9697	8.361	5.474
EMD-AHA-BP	0.9717	8.156	5.249
CEEMDAN-AHA-BP	0.9738	7.636	4.670

According to Table 4, the CEEMDAN-AHA-BP model produces the maximum  $R^2$  value, while the minimum values for the other evaluations. This shows the best performance of the CEEMDAN-AHA-BP model. The change from BP to PSO-BP to AHA-BP shows that the use of algorithms can enhance the performance of predictive models. Meanwhile, the use of signal processing techniques such as EMD can also improve the model's accuracy.

## 4 Uncertainty Analysis

### 4.1 Nonparametric Kernel Density Estimation

This study quantifies the probability distribution of predicted PV power using NPKDE and confidence intervals. This accurate prediction and uncertainty analysis helps to realize the effective use of clean energy and promotes the development of energy systems in a more sustainable direction. The NPKDE

does not require the assumption of a distribution, but it does need to select a kernel function. Different kernel functions have different distributions. The Gaussian kernel function has a wide range of applicability and high accuracy, so this kernel function is employed in the study.

The Gaussian kernel function is described in Equation (13):

$$g(x) = \frac{1}{\sqrt{2\pi}\sigma} \exp\left(-\frac{(x-u)^2}{2\sigma^2}\right) \quad (13)$$

where  $u$  is the average of the PV prediction error and  $\sigma$  is the standard deviation.

The NPKDE calculates the probability distribution of the prediction error as follows:

$$f(x) = \frac{1}{N} \sum_{i=1}^N g\left(\frac{x-x_i}{h}\right) \quad (14)$$

where  $N$  means the amount of data points in the PV power prediction error interval,  $x_i$  donates the  $i$ th sample, and  $h$  means the bandwidth coefficient.

#### 4.2 NPKDE-based Confidence Intervals Comparative Analysis of Prediction Models

In this work, the NPKDE is utilized to generate the probability density of PV power forecasts, and then confidence intervals are established based on the probability density distribution for quantitative analysis. The following is the PV power error  $e$ .

$$e = P_{pre} - P_{act} \quad (15)$$

where  $P_{pre}$  is the power prediction value and  $P_{act}$  is the actual value.

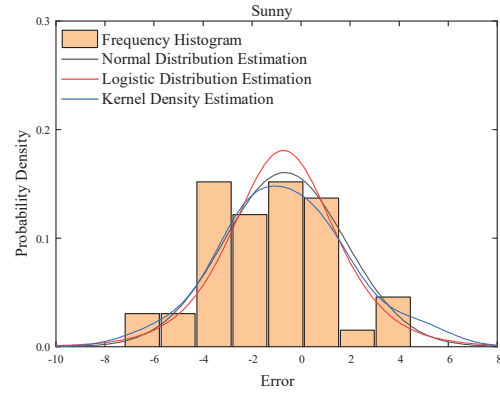
According to PV power error, the confidence level calculated below:

$$P(e_{low} < e < e_{up}) = 1 - \theta \quad (16)$$

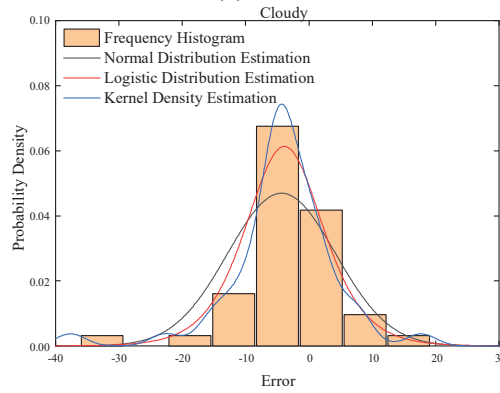
where  $P(e_{low} < e < e_{up})$  represents the confidence interval,  $1 - \theta$  is the confidence level,  $e_{up}$  and  $e_{low}$  stand for the confidence interval's upper and lower bounds, respectively. Due to the above equation, the upper and lower limits of the prediction interval are  $[P_{pre} - e_{up}, P_{pre} - e_{low}]$ .

#### 4.3 Probability Density Estimates and Confidence Intervals for Prediction Errors

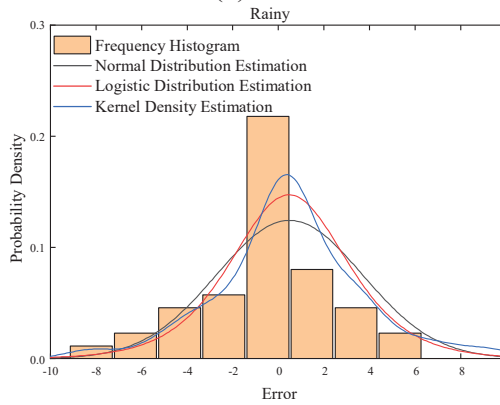
The uncertainty analysis of the predicted power is discussed according to three different types of weather: sunny, cloudy, and rainy. The prediction



(a)



(b)



(c)

**Figure 8** Probability density distribution chart: (a) Sunny; (b) Cloudy; (c) Rainy.

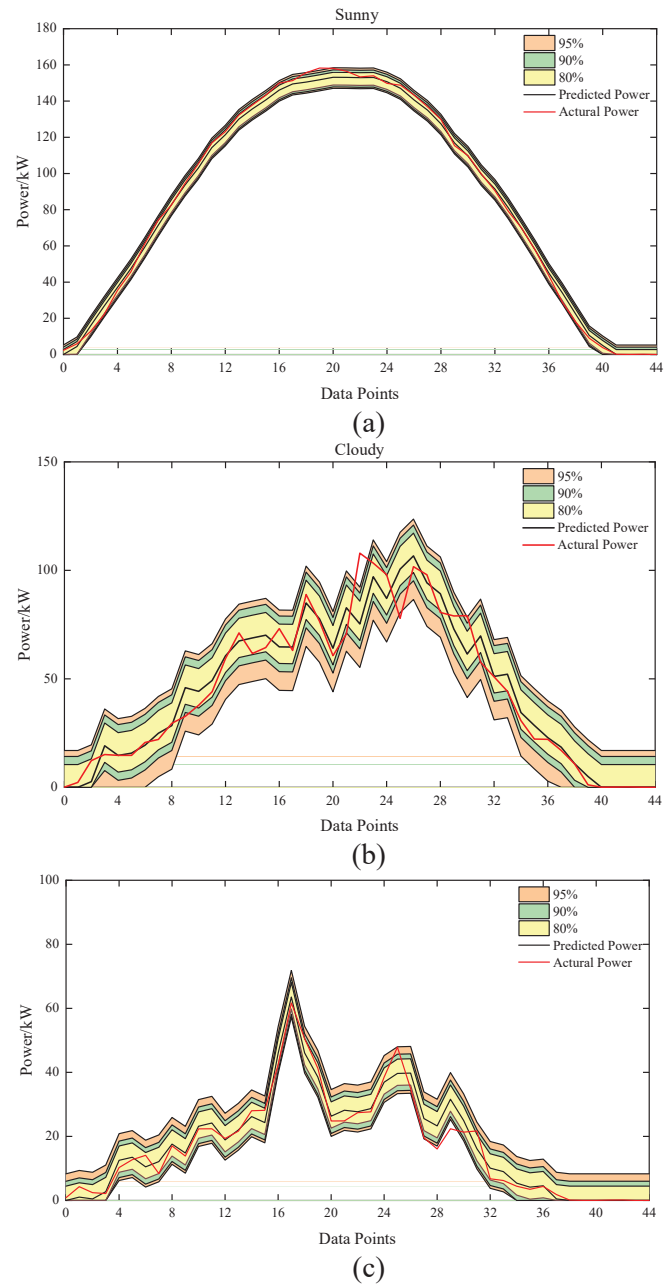


**Figure 9** Confidence interval diagram: (a) Sunny; (b) Cloudy; (c) Rainy.



error of the CEEMDAN-AHA-BP model is analyzed using NPKDE. To test the reliability of the method, normal and logistic distributions are selected for comparison. The distribution of the probability density curves of three methods for the prediction error of this model is illustrated in Figure 8.

From Figure 8, the probability density curve of KDE most closely approximates the actual distribution under the three weather conditions. The normal distribution has the worst-fitted effect. The prediction errors for the three weather conditions are mainly concentrated in the range of  $-10$  kW to  $10$  kW. However, there are also a small number of points with large errors, and there are points with absolute errors up to  $30$  kW on cloudy days. When the probability density distribution of the prediction error is computed utilizing NPKDE, the confidence intervals are used to quantify the uncertainty distribution of PV power prediction. The distribution of confidence intervals for the proposed prediction model at 95%, 90% and 80% confidence levels are shown in Figure 9.

According to the analysis of Figure 9 above, as can be seen, some of the actual data points are not included in the confidence interval under different weather conditions, especially under cloudy conditions. However, the overall probability of the actual PV power is higher with respect to the confidence level.

The evaluation indicators for uncertainty analysis of PV predicted power are Prediction Interval Coverage Probability (PICP) and Prediction Interval Average Width (PINAW). In this paper, only one of the PICP is selected for assessment, and the formula is as follows:

$$PICP = \frac{1}{N} \sum_{i=1}^N \lambda_i \times 100\% \quad (17)$$

If a point of the actual value falls within the confidence interval,  $\lambda_i$  is 1, otherwise it is 0. Table 5 displays the coverage of confidence intervals under various weather conditions. The table verifies the accuracy of the NPKDE for quantitative analysis of confidence intervals.

**Table 5** Confidence level results

Weather Conditions	Confidence Level		
	80%	90%	95%
Sunny	80.00%	93.33%	97.78%
Cloudy	80.00%	86.67%	93.33%
Rainy	84.44%	91.11%	95.56%

## 5 Conclusions

As the variability behaviour of PV power generation impacts the stability of the power system, short-term PV forecasts are of great significance for scheduling in conventional power systems as well as in PV-ESS. In the work, a PV power prediction model is introduced with CEEMDAN decomposition and AHA-BP, and the accuracy in predicting is confirmed by taking one month of meteorological data and historical PV power as an example and comparing it with other models. The conclusions of this article can be summarized as below:

- (1) The utilization of CEEMDAN method improves the accuracy of the AHA-BP model in PV power prediction. PV power prediction model performance can be improved with a combination of optimization algorithms and signal processing techniques.
- (2) The AHA has a stronger global search capability than the PSO. In addition, by combining the optimization algorithm with the neural network, it can help the model from being trapped in the local optimal solution, thus enhancing its stability.
- (3) NPKDE provides an accurate calculation of the probability density distribution of prediction error.

Since the CEEMDAN-AHA-BP model involves signal decomposition, optimization algorithms, and neural network models, the algorithm has high complexity and requires high computational resources and time costs. The training of the algorithm takes a lot of historical data and requires extremely precise and superior information, which may be difficult to fulfill in some cases. In the future, the performance of the CEEMDAN-AHA-BP model in PV power prediction can be further strengthened by the optimization and improvement of the algorithm, combined with other prediction techniques, and by improving the quality of data through data processing methods. It provides more accurate support for the real-time dispatch of renewable energy generation systems.

## Acknowledgments

This research was funded by Xiamen University of Technology scientific research project, Research on key technology of “source-network-load” electric-carbon coupling optimized operation in active distribution networks, grant number YKJ22020R and the Natural Science Foundation of Fujian

Province, China (Grant No. 2022J05284), Research on key technologies of intelligent diagnosis and monitoring considering distributed photovoltaic generation.

## References

- [1] L. Liu et al., 'Prediction of short-term PV power output and uncertainty analysis', *Applied Energy*, vol. 228, pp. 700–711, October 2018,
- [2] M. Manas, 'Optimization of Distributed Generation Based Hybrid Renewable Energy System for a DC Micro-Grid Using Particle Swarm Optimization', *Distributed Generation & Alternative Energy Journal*, pp. 7–25, October 2018,
- [3] M. Li, W. Wang, Y. He, and Q. Wang, 'Deep learning model for short-term photovoltaic power forecasting based on variational mode decomposition and similar day clustering', *Computers and Electrical Engineering*, vol. 115, p. 109116, April 2024,
- [4] A. T. Eseye, J. Zhang, and D. Zheng, 'Short-term photovoltaic solar power forecasting using a hybrid Wavelet-PSO-SVM model based on SCADA and Meteorological information', *Renewable Energy*, vol. 118, pp. 357–367, April 2018,
- [5] S. Han, Y. Qiao, J. Yan, Y. Liu, L. Li, and Z. Wang, 'Mid-to-long term wind and photovoltaic power generation prediction based on copula function and long short term memory network', *Applied Energy*, vol. 239, pp. 181–191, April 2019,
- [6] R. Liu, J. Wei, G. Sun, S. M. Mueen, S. Lin, and F. Li, 'A short-term probabilistic photovoltaic power prediction method based on feature selection and improved LSTM neural network', *Electric Power Systems Research*, vol. 210, p. 108069, September 2022,
- [7] B. Gu, H. Shen, X. Lei, H. Hu, and X. Liu, 'Forecasting and uncertainty analysis of day-ahead photovoltaic power using a novel forecasting method', *Applied Energy*, vol. 299, p. 117291, October 2021,
- [8] H. Zhou, Y. Zhang, L. Yang, Q. Liu, K. Yan, and Y. Du, 'Short-Term Photovoltaic Power Forecasting Based on Long Short Term Memory Neural Network and Attention Mechanism', *IEEE Access*, vol. 7, pp. 78063–78074, 2019,
- [9] Y.-K. Wu, C.-L. Huang, Q.-T. Phan, and Y.-Y. Li, 'Completed Review of Various Solar Power Forecasting Techniques Considering Different Viewpoints', *Energies*, vol. 15, no. 9, p. 3320, May 2022,

- [10] C. Zhang, T. Peng, and M. S. Nazir, 'A novel integrated photovoltaic power forecasting model based on variational mode decomposition and CNN-BiGRU considering meteorological variables', *Electric Power Systems Research*, vol. 213, p. 108796, December 2022,
- [11] Y. K. Semero, J. Zhang, D. Zheng, and D. Wei, 'A GA-PSO hybrid algorithm based neural network modeling technique for short-term wind power forecasting', *Distributed Generation & Alternative Energy Journal*, vol. 33, no. 4, pp. 26–43, 2018.
- [12] Y. Liang, L. Zhi, and Y. Haiwei, 'Medium-term Load Forecasting Method with Improved Deep Belief Network for Renewable Energy', *Distributed Generation & Alternative Energy Journal*, pp. 485–500, 2022,
- [13] Y. Li, L. Zhou, P. Gao, B. Yang, Y. Han, and C. Lian, 'Short-Term Power Generation Forecasting of a Photovoltaic Plant Based on PSO-BP and GA-BP Neural Networks', *Front. Energy Res.*, vol. 9, p. 824691, January 2022,
- [14] W. Zhao, L. Wang, and S. Mirjalili, 'Artificial hummingbird algorithm: A new bio-inspired optimizer with its engineering applications', *Computer Methods in Applied Mechanics and Engineering*, vol. 388, p. 114194, January 2022,
- [15] N. Belbachir, S. Kamel, M. H. Hassan, and M. Zellagui, 'Optimizing energy management of hybrid wind generation-battery energy storage units with long-term memory artificial hummingbird algorithm under daily load-source uncertainties in electrical networks', *Journal of Energy Storage*, vol. 78, p. 110288, 2024.
- [16] L. Feng, Y. Zhou, Q. Luo, and Y. Wei, 'Complex-valued artificial hummingbird algorithm for global optimization and short-term wind speed prediction', *Expert Systems with Applications*, vol. 246, p. 123160, July 2024,
- [17] M. Ebeed et al., 'A Modified Artificial Hummingbird Algorithm for solving optimal power flow problem in power systems', *Energy Reports*, vol. 11, pp. 982–1005, June 2024,
- [18] H. Liu, H. Tian, and Y. Li, 'Comparison of new hybrid FEEMD-MLP, FEEMD-ANFIS, Wavelet Packet-MLP and Wavelet Packet-ANFIS for wind speed predictions', *Energy Conversion and Management*, vol. 89, pp. 1–11, 2015.
- [19] Y. Ding, Z. Chen, H. Zhang, X. Wang, and Y. Guo, 'A short-term wind power prediction model based on CEEMD and WOA-KELM', *Renewable Energy*, vol. 189, pp. 188–198, 2022.

- [20] H. Sun, Q. Cui, J. Wen, L. Kou, and W. Ke, 'Short-term wind power prediction method based on CEEMDAN-GWO-Bi-LSTM', *Energy Reports*, vol. 11, pp. 1487–1502, 2024.
- [21] J. Wang, Y. Yu, B. Zeng, and H. Lu, 'Hybrid ultra-short-term PV power forecasting system for deterministic forecasting and uncertainty analysis', *Energy*, vol. 288, p. 129898, February 2024,
- [22] K. N. Zhao, T. J. Pu, X. Y. Wang, and Y. Li, 'Probabilistic forecasting for photovoltaic power based on improved bayesian neural network', *Power System Technology*, vol. 43, no. 12, pp. 4377–4386, 2019.
- [23] Songjian Chai, Ming Niu, Z. Xu, Loi Lei Lai, and K. P. Wong, 'Nonparametric conditional interval forecasts for PV power generation considering the temporal dependence', in *2016 IEEE Power and Energy Society General Meeting (PESGM)*, Boston, MA, USA: IEEE, July 2016, pp. 1–5.
- [24] Y. Han, N. Wang, M. Ma, H. Zhou, S. Dai, and H. Zhu, 'A PV power interval forecasting based on seasonal model and nonparametric estimation algorithm', *Solar Energy*, vol. 184, pp. 515–526, May 2019,
- [25] N. E. Huang et al., 'The empirical mode decomposition and the Hilbert spectrum for nonlinear and non-stationary time series analysis', *Proc. R. Soc. Lond. A*, vol. 454, no. 1971, pp. 903–995, March 1998,
- [26] K. Bian and Z. Wu, 'Data-based model with EMD and a new model selection criterion for dam health monitoring', *Engineering Structures*, vol. 260, p. 114171, June 2022,
- [27] A. Gupta, S. Sharma, and S. Saroha, 'A new hybrid short term solar irradiation forecasting method based on CEEMDAN decomposition approach and BiLSTM deep learning network with grid search algorithm', *Distributed Generation & Alternative Energy Journal*, pp. 1073–1118, 2023.
- [28] H. Yang, X. Yang, and G. Li, 'Forecasting carbon price in China using a novel hybrid model based on secondary decomposition, multi-complexity and error correction', *Journal of Cleaner Production*, vol. 401, p. 136701, May 2023,
- [29] P. Ran, K. Dong, X. Liu, and J. Wang, 'Short-term load forecasting based on CEEMDAN and Transformer', *Electric Power Systems Research*, vol. 214, p. 108885, 2023.
- [30] A. Alruban, H. A. Mengash, M. M. Eltahir, N. S. Almalki, A. Mahmud, and M. Assiri, 'Artificial Hummingbird Optimization Algorithm With Hierarchical Deep Learning for Traffic Management in Intelligent Transportation Systems', *IEEE Access*, 2024.

- [31] A. Ramadan, 'Optimal allocation of renewable DGs using artificial hummingbird algorithm under uncertainty conditions', *Ain Shams Engineering Journal*, 2023.
- [32] G. Chen, B. Tang, X. Zeng, P. Zhou, P. Kang, and H. Long, 'Short-term wind speed forecasting based on long short-term memory and improved BP neural network', *International Journal of Electrical Power & Energy Systems*, vol. 134, p. 107365, January 2022,
- [33] Y. Nie, P. Jiang, and H. Zhang, 'A novel hybrid model based on combined preprocessing method and advanced optimization algorithm for power load forecasting', *Applied Soft Computing*, vol. 97, p. 106809, December 2020,

## Biographies



**Zhiyuan Zeng** graduated from Xiamen University of Technology in 2021. He is currently studying for a master's degree at Xiamen University of Technology. The main research directions include photovoltaic power prediction.



**Tianyou Li** graduated from Fuzhou University. His master's degree and PhD in electrical engineering were obtained at North China Electric Power

University. 2019.7 Teaching at School of Electrical Engineering and Automation, Xiamen University of Technology. The main research directions include photovoltaic power prediction and intelligent power distribution technology.



**Jun Su** graduated in Electrical Engineering from Staffordshire University in 2012 and a master's degree in electrical energy systems from Cardiff University in 2014. 2017.10–2020.12 Studied at Auckland University of Technology, New Zealand, and obtained a PhD in Electrical engineering. 2021.7 Teaching at School of Electrical Engineering and Automation, Xiamen University of Technology. The main research directions include electric vehicles and new energy grid optimization, intelligent distribution network, relay protection.



**Yihan Yang** graduated from Xiamen University of Technology in 2023. He is currently studying for a master's degree at Xiamen University of Technology. The main research directions include photovoltaic power prediction.



**Yajun Lin** graduated from Xiamen University of Technology in 2023. He is currently studying for a master's degree at Xiamen University of Technology. The main research directions include photovoltaic power prediction.